

Surface Science Letters

Surface structure and relaxation at the Pt₃Sn(1 1 1)/electrolyte interface

M.E. Gallagher ^a, C.A. Lucas ^{a,*}, V. Stamenković ^b, N.M. Marković ^b,
P.N. Ross ^b

^a Oliver Lodge Laboratory, Department of Physics, University of Liverpool, Oxford Street, Liverpool L69 7ZE, UK

^b Materials Science Division, Lawrence Berkeley National Laboratory, University of California, Berkeley, CA 94720, USA

Received 2 April 2003; accepted for publication 27 August 2003

Abstract

In situ surface X-ray scattering (SXS) measurements have been performed to determine the surface structure of Pt₃Sn(1 1 1) in sulfuric acid electrolyte. Potentiodynamic measurements indicate that the ultra high vacuum (UHV) prepared $p(2 \times 2)$ alloy surface structure is stable upon transfer to electrolyte and remains stable during subsequent cycling of the applied potential. A detailed structural study by crystal truncation rod (CTR) analysis shows that the surface layer of Pt and Sn atoms undergoes an expansion of $\sim 2\%$ of the (1 1 1) layer spacing at low potential (0.05 V vs. reversible hydrogen electrode) in CO-free electrolyte. At 0.55 V the expansion of the Pt atoms is reduced to $\sim 0.6\%$, whereas the Sn atoms are expanded by $\sim 6\%$ of the layer spacing. The potential-induced buckling of the surface layer is also observed in CO-saturated electrolyte and is a precursor to Sn dissolution which occurs at ~ 1.0 V, causing irreversible roughening of the surface.

© 2003 Elsevier B.V. All rights reserved.

Keywords: X-ray scattering, diffraction, and reflection; Catalysis; Surface relaxation and reconstruction; Alloys; Solid–liquid interfaces

1. Introduction

Recent studies have shown that bimetallic alloy surfaces can enhance the oxidation of CO and small organic molecules due to a combination of bifunctional and electronic (or ligand) effects. Binary alloys composed of platinum and an electropositive metal are of interest since they often

form compounds with ordered structures at characteristic bulk compositions and may have ordered surface structures with unique catalytic properties. The existence of both metals at the surface can greatly affect the catalytic and adsorptive processes occurring at the interface in comparison to a pure Pt electrode. The study of Pt₃Sn as a model electrocatalyst is, therefore, an important step towards the fundamental physical understanding of catalysis by alloys, particularly as it has one of the highest catalytic activities for CO electrooxidation recorded to date [1]. Whilst Pt₃Sn has been investigated theoretically [2,3] and in ultra high vacuum

* Corresponding author. Tel.: +44-151-794-3361; fax: +44-151-794-3441.

E-mail address: clucas@liv.ac.uk (C.A. Lucas).

(UHV) [4–8] there has been no in situ surface atomic structure characterisation exploring surface reactions at the interface and how they govern the surface structure.

In this letter we describe an in situ surface X-ray scattering (SXS) study of the $\text{Pt}_3\text{Sn}(1\ 1\ 1)$ electrode in sulfuric acid solution. Potentiodynamic measurements involving the monitoring of X-ray diffraction features due to the $\text{Pt}_3\text{Sn}(1\ 1\ 1)$ structure during cycling of the applied potential have been performed to determine the potential window of stability of the surface and to follow the potential dependence of the outermost atomic layer expansion. Further to this a detailed characterisation of the surface structure at fixed potentials of interest is presented in the form of crystal truncation rod (CTR) analysis, with and without carbon monoxide adsorbed on the surface. Results obtained indicate that the $p(2\times 2)$ surface structure shown in Fig. 1(b), which is simply the bulk termination of the alloy and is prepared under UHV conditions, can be transferred to an electrochemical environment and remains stable when subsequently cycling the potential from the onset of hydrogen evolution to the onset of Sn dissolution. This structural model reveals the surface relaxation that occurs during the adsorption/desorption of hydrogen, sulfate molecules, carbon monoxide and the onset of Sn dissolution.

2. Experimental details

The preparation of the $\text{Pt}_3\text{Sn}(1\ 1\ 1)$ single crystal (miscut $< 0.2^\circ$) was performed under UHV conditions by continued cycles of sputtering and annealing until a clean surface is produced [9]. Low energy electron diffraction patterns showed the characteristic $p(2\times 2)$ structure consistent with bulk termination of the $(1\ 1\ 1)$ crystal surface. For transportation purposes the crystal was transferred from the UHV chamber into clean deaerated water. Under these conditions the surface remains free from contaminants as confirmed both by emersion back into the UHV environment and by the electrochemical response of the surface which is sensitive to impurity concentrations. The crystal was then transferred to the electrochemical

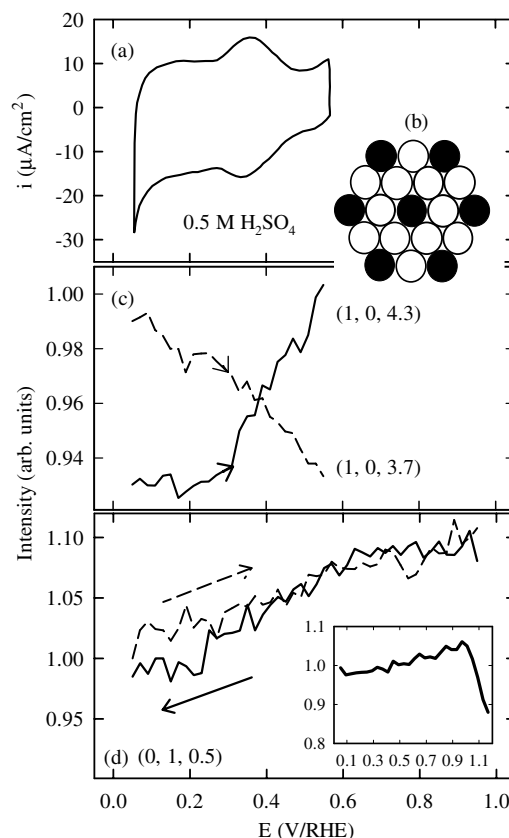


Fig. 1. (a) Cyclic voltammetry of $\text{Pt}_3\text{Sn}(1\ 1\ 1)$ in $0.5\ \text{M}\ \text{H}_2\text{SO}_4$, (b) $p(2\times 2)$ surface structure with Pt surface atoms represented by white circles and Sn atoms as black circles, (c) X-ray voltammetry (XRV) measured at $(1, 0, 3.7)$ and $(1, 0, 4.3)$, positions which are sensitive to surface expansion effects in $0.5\ \text{M}\ \text{H}_2\text{SO}_4$ and (d) XRV measured in CO-saturated electrolyte at the “anti-Bragg” position $(0, 1, 0.5)$ showing reversible potential-dependent changes until the surface is irreversibly roughened above $0.9\ \text{V}$ (inset).

X-ray cell [10] with a drop of ultra pure water protecting the surface and was immersed at open circuit potential in $0.5\ \text{M}\ \text{H}_2\text{SO}_4$. The experimental procedure followed that of similar experiments reported previously [10–12]. X-ray measurements were performed on beamline 7–2 at the Stanford Synchrotron Research Laboratory (SSRL) using a $10\ \text{keV}$ X-ray beam, defined by slits to be a $1\ \text{mm}\times 1\ \text{mm}$ spot incident on the sample. The in-plane resolution of the diffractometer was defined by Soller slits to be $\sim 0.005\ \text{\AA}^{-1}$. Additional measurements were performed on the XMaS

beamline (BM28) at the European Synchrotron Radiation Facility (ESRF) [13]. The crystal was indexed to a conventional hexagonal unit cell for a fcc (1 1 1) surface, e.g. Pt(1 1 1), where the surface normal is along the $(0, 0, l)_{\text{hex}}$ direction and the $(h, 0, 0)_{\text{hex}}$ and $(0, k, 0)_{\text{hex}}$ directions lie in the surface plane. The lattice parameter of $\text{Pt}_3\text{Sn}(1\ 1\ 1)$ was taken as 3.993 Å, as determined during the X-ray diffraction experiments. The alloy superlattice gives rise to additional scattering features at half-integer $(h\ k\ l)$ positions compared to a single crystal fcc metal, as will be discussed below in relation to the CTR data. The outer chamber of the X-ray cell was continuously purged with nitrogen to protect the Pt_3Sn surface from oxygen. For measurements of CO adsorption and oxidation the outer cell was purged with high purity CO (Matheson, 99.999% purity) which can diffuse into the electrolyte. The reference electrode used in the X-ray cell was a saturated calomel electrode, however all potentials in this paper are quoted vs. the reversible hydrogen electrode.

3. Results and discussion

A representative cyclic voltammogram for the $\text{Pt}_3\text{Sn}(1\ 1\ 1)$ surface in 0.5 M H_2SO_4 is shown in Fig. 1(a). The potential region from ~ 0.05 to 0.2 V corresponds to hydrogen adsorption/desorption onto the surface Pt adsorption sites. In the potential region ~ 0.35 –0.6 V a reversible feature is observed which has been assigned to the adsorption/desorption of bisulfate anions on Pt sites on the basis of Fourier Transform Infra Red Spectroscopy measurements [14]. In these measurements the upper potential limit was restricted to 0.6 V in order to prevent Sn dissolution. Having reproduced the cyclic voltammetry shown in Fig. 1(a) in the X-ray cell, it is possible to proceed with X-ray measurements confident that the electrolyte is free from contamination. The potential dependence of the $\text{Pt}_3\text{Sn}(1\ 1\ 1)$ electrode surface was thus monitored by X-ray voltammetry (XRV). Fig. 1(c) shows the change in diffracted intensity at two reciprocal lattice positions, $(1, 0, 3.7)$ and $(1, 0, 4.3)$, on the $(1, 0, l)$ CTR. These positions are chosen as they are typically sensitive to lattice surface ex-

pansion effects; surface expansion causes an asymmetry in the intensity around the $(1, 0, 4)$ Bragg reflection and so an increase in the intensity at $(1, 0, 3.7)$ is accompanied by a decrease at $(1, 0, 4.3)$ and vice versa [15]. As the potential is cycled from 0.05 to 0.55 V there is a decrease in the intensity at $(1, 0, 3.7)$ with a corresponding increase in the intensity at $(1, 0, 4.3)$. Such behavior is consistent with a change in the expansion of the surface Pt and Sn atoms as observed previously for pure Pt single crystal electrodes [15].

To characterize the surface expansion indicated by the XRV results in Fig. 1(c), a detailed surface X-ray diffraction study was performed. This involved measurement and modeling of the CTR's that arise due to the termination of the bulk lattice [16]. As a result of a doubling of the conventional fcc unit cell size due to the alloy there are both half-integer and integer CTR's. Fig. 2 shows the CTR data measured at 0.05 V. The data points shown as circles represent background-subtracted

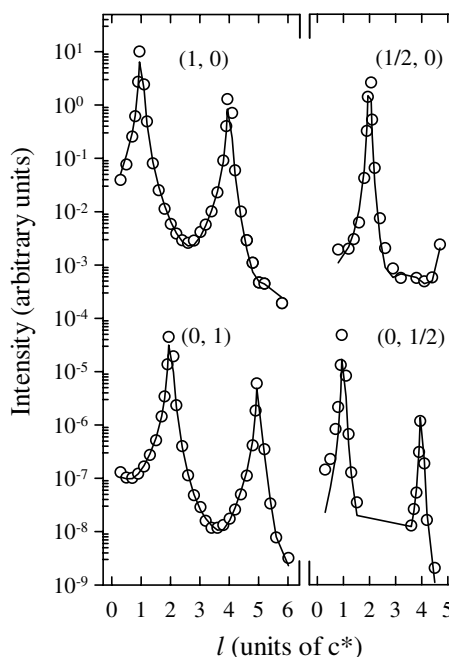


Fig. 2. Crystal truncation rod (CTR) data for the $\text{Pt}_3\text{Sn}(1\ 1\ 1)$ surface with the applied potential held at 0.05 V. The $p(2 \times 2)$ superlattice gives rise to fractional order CTR's (right), at half integer positions. The solid line is a best fit to the data allowing for independent relaxation of the surface Pt and Sn atoms.

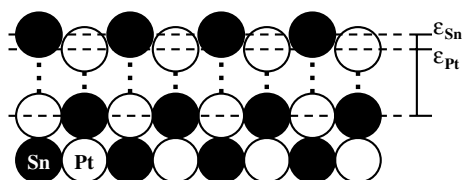


Fig. 3. Structural model of the $\text{Pt}_3\text{Sn}(111)$ surface used for modeling the CTR data. The structural parameters included for the best fit allow for independent variation in the surface atomic layer expansions (ϵ_{Sn} , ϵ_{Pt}), coverage (θ_{Sn} , θ_{Pt}) and roughness (σ_{Sn} , σ_{Pt}). The surface expansion is exaggerated for clarity.

integrated intensities obtained from rocking scans at each point, l , along the CTR's. The solid line through the data points corresponds to a best fit to the data using the structural model shown in Fig. 3. The CTR data are modeled using kinematical X-ray diffraction theory [16,17] whereby the fcc (111) unit cell is doubled in size to match the unit cell of $\text{Pt}_3\text{Sn}(111)$. The best fit to the CTR data was obtained using a least-squares method in which the variable structural parameters were the surface atomic layer expansion (ϵ_{Sn} , ϵ_{Pt}), surface coverage (θ_{Sn} , θ_{Pt}) and surface roughness (σ_{Sn} , σ_{Pt}). The fit parameters obtained have been summarized in Table 1. Fits to the data at 0.05 V indicate that adsorption of hydrogen on the surface at this potential has caused the Pt atoms to expand by 2.3% of the (111) layer spacing whereas the surface Sn atoms are expanded by 1.8%. These values are similar to the surface expansion observed with a pure Pt(111) single crystal in the hydrogen absorption region [11]. The CTR measurements were repeated at 0.55 V producing data that was very similar to that shown in Fig. 2. At this potential hydrogen adsorbed on the surface has been replaced by sulfate anions. Shown in Fig. 4 is the

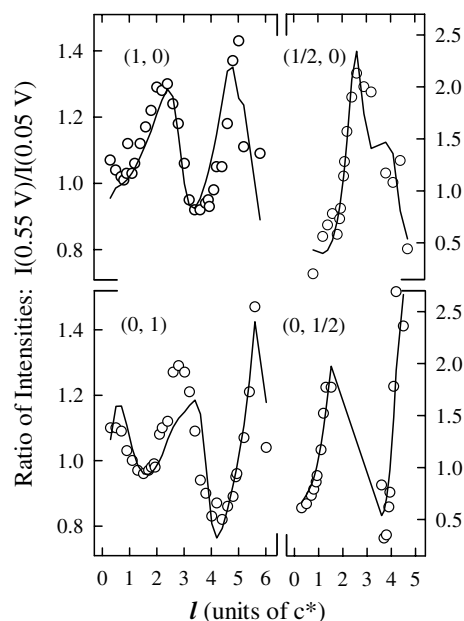


Fig. 4. Ratio plots of CTR data, i.e. $I_{0.55\text{ V}}/I_{0.05\text{ V}}$. The solid line is a best fit to the ratio data set allowing variation in the surface atomic layer expansions, coverage and roughness (see text for details).

ratio of the diffracted intensity of the CTR data set at 0.55 V to that at 0.05 V. The asymmetry around the position of the Bragg peaks visible on the plot is indicative of changes in the surface expansion. The ratio data set was modeled allowing for variation in the same structural parameters used for the CTR data. The best fit to the ratio data set (see Table 1) indicated that, while there is no change in the surface coverage and roughness of the Pt and Sn atoms, the expansion of surface Pt is reduced to 0.6%. In contrast to this, the surface Sn atoms undergo a large expansion of $(0.15 \pm 0.02 \text{ \AA})$ or

Table 1

Best fit parameters obtained from analysis of CTR data taken at 0.05 V and 0.55 V in CO-free and CO-saturated electrolyte. The fit parameters deduced for the surface atomic layer expansion (ϵ_{Sn} , ϵ_{Pt}), relative surface coverage (θ_{Sn} , θ_{Pt}) and surface roughness (σ_{Sn} , σ_{Pt}) are shown along with their associated error

		ϵ_{Pt} (%)	ϵ_{Sn} (%)	θ_{Pt}	θ_{Sn}	σ_{Pt} (Å)	σ_{Sn} (Å)
N	0.05 V	2.3 ± 0.5	1.8 ± 0.4	0.60 ± 0.03	0.20 ± 0.03	0.11 ± 0.02	0.31 ± 0.04
	0.55 V	0.6 ± 0.4	6.5 ± 0.8	0.62 ± 0.02	0.22 ± 0.01	0.12 ± 0.01	0.33 ± 0.01
CO	0.05 V	1.5 ± 0.4	1.6 ± 0.4	0.59 ± 0.03	0.20 ± 0.03	0.13 ± 0.02	0.29 ± 0.04
	0.55 V	1.5 ± 0.4	5.1 ± 0.5	0.61 ± 0.02	0.18 ± 0.01	0.14 ± 0.01	0.24 ± 0.01

6.5% of the bulk lattice spacing. This shows that at positive potential the surface becomes increasingly buckled as the Sn atoms expand outwards.

It is now well established that Pt_3Sn is one of the best catalysts for bulk CO electrooxidation, having a positive reaction order with respect to CO partial pressure. Due to the wide potential region over which CO oxidation occurs on $\text{Pt}_3\text{Sn}(111)$, it is impossible in the polarization curve for CO oxidation to isolate the possible contribution of Sn dissolution from the surface. As shown above, CTR measurements are sensitive to the termination of the Pt_3Sn lattice and can therefore be used to examine the stability of the surface during the adsorption and oxidation of CO. With a constant overpressure of CO in the cell, CO displaces hydrogen from the surface Pt atoms as observed on the pure $\text{Pt}(111)$ electrode [12]. At 0.05 V CO was strongly adsorbed onto $\text{Pt}(111)$, forming a compact $p(2 \times 2)$ -3CO overlayer and causing a large (4%) expansion of the surface atoms. In the case of $\text{Pt}_3\text{Sn}(111)$ we were unable to observe any diffraction peaks due to an ordered CO adlayer. Furthermore, CTR measurements (not shown here) gave an identical expansion of the surface Pt and Sn atoms by 1.5% of the (111) layer spacing. If the Pt expansion is proportional to the strength of adsorption of CO then this implies that CO is only weakly adsorbed on $\text{Pt}_3\text{Sn}(111)$. This proposition is in agreement with recent theoretical calculations which showed that the binding energy of CO on $\text{Pt}_3\text{Sn}(111)$ was 0.2 eV lower than on $\text{Pt}(111)$ [3].

XRV measurements were performed as the electrode potential was cycled from 0.05 to 0.55 V in CO-saturated electrolyte and the results were similar to those shown in Fig. 1(c) although the potential-dependent changes in the X-ray intensities were considerably smaller than in CO-free electrolyte. CTR data were measured at 0.55 V and a fit to a ratio data set (as in Fig. 4) gave an expansion of the surface Pt atoms by 1.5% (identical to that observed at 0.05 V), whereas the surface Sn atom expansion was similar to that observed in CO-free solution. There were no other significant changes in the fit parameters. At 0.55 V it is expected that the surface is still populated with CO due to continuous adsorption from the CO-saturated electrolyte (the steady state coverage is un-

known but the current for CO oxidation implies continuous adsorption of CO). Fig. 1(d) shows the XRV measured at (0, 1, 0.5), an ‘anti-Bragg’ position which is sensitive to the surface termination of the Pt_3Sn lattice, as the potential was cycled up to 0.95 V. The solid and dashed lines show that there is a continuous reversible change in the X-ray diffraction over this potential range. Upon cycling to more positive potentials (>1.0 V), however, the diffracted intensity reduces greatly, as shown inset to Fig. 1(d). This is due to dissolution of Sn from the surface which leads to irreversible roughening of the electrode. The XRV measurements demonstrate that the $\text{Pt}_3\text{Sn}(111)$ surface is stable up to 0.95 V during the electrooxidation of CO. Consequently, the current measured in the polarization curve [1] is entirely due to the oxidation of CO (the current due to OH adsorption is negligible contributing to pseudocapacitance rather than giving faradaic curves).

In summary, a detailed in situ characterisation of the $\text{Pt}_3\text{Sn}(111)$ /electrolyte interface using surface X-ray diffraction techniques has been presented. The results indicate that it is possible to prepare a good quality alloy surface in UHV and preserve the surface structure during transfer to an electrochemical environment. Potentiostatic structural studies by CTR analysis have shown that hydrogen adsorption onto the Pt atoms (at 0.05 V) induces a $\sim 2\%$ expansion of the Pt_3Sn surface layer. At positive potential (0.55 V), with sulfate adsorbed on the surface, the surface becomes increasingly buckled with the Sn surface atoms moving outwards by 6.5% of the lattice spacing. Similar results are also observed in CO-saturated electrolyte. Remarkably the $\text{Pt}_3\text{Sn}(111)$ surface is stable up to 0.95 V in CO-saturated solution. The buckling of the surface layer is a precursor to dissolution of Sn into the electrolyte.

Acknowledgements

This work was supported by the Director, Office of Science, Office of Basic Energy Sciences, Materials Science Division (MSD), US Department of Energy (DOE) under contract no. DE-AC03-76SF00098. Research was carried out in part at

SSRL, which is funded by the Division of Chemical Sciences (DCS), U.S. DOE. Additional research was performed on the EPSRC funded XMaS CRG beamline (BM 28) at the ESRF, Grenoble. CAL would like to acknowledge the support of an EPSRC Advanced Research Fellowship. MEG acknowledges the support of an EPSRC studentship.

References

- [1] H.A. Gasteiger, N.M. Marković, P.N. Ross, *Catal. Lett.* 36 (1996) 1.
- [2] Š. Pick, *Surf. Sci.* 436 (1999) 220.
- [3] T.E. Shubina, M.T.M. Koper, *Electrochim. Acta* 47 (2002) 3621.
- [4] A. Atrei, U. Bardi, G. Roviola, M. Torrini, E. Zanazzi, P.N. Ross, *Phys. Rev. B.* 46 (1992) 1649.
- [5] U. Bardi, *Rep. Prog. Phys.* 57 (1994) 939.
- [6] W.C.A.N. Ceelen, *Surf. Sci.* 406 (1998) 264.
- [7] C. Xu, B.E. Koel, *Surf. Sci.* 304 (1994) L505.
- [8] D.I.J. Jerdev, B.E. Koel, *Surf. Sci.* 492 (2001) 106.
- [9] H.A. Gasteiger, N.M. Marković, P.N. Ross, *J. Phys. Chem.* 99 (1995) 8945.
- [10] I.M. Tidswell, N.M. Marković, C.A. Lucas, P.N. Ross, *Phys. Rev. B.* 47 (1993) 16542.
- [11] C.A. Lucas, N.M. Marković, P.N. Ross, *Surf. Sci.* 425 (1999) L381.
- [12] C.A. Lucas, N.M. Marković, P.N. Ross, *Surf. Sci.* 448 (2000) 77.
- [13] S. Brown et al., *J. Synch. Rad.* 8 (2001) 1172.
- [14] V. Stamenković, M. Arenz, C.A. Lucas, M.E. Gallagher, P.N. Ross, N.M. Marković, *J. Am. Chem. Soc.* 125 (2003) 2736.
- [15] C.A. Lucas, *Electrochim. Acta.* 47 (2002) 3065.
- [16] I.K. Robinson, D.J. Tweet, *Rep. Prog. Phys.* 55 (1992) 599.
- [17] C.A. Lucas, N.M. Marković, in: *Encyclopedia of Electrochemistry*, vol. 2, Wiley-VCH, 2003, Section 4.1.2.1.2.